

**TITLE**

The terrestrial biosphere as a net source of greenhouse gases to the atmosphere

**AUTHORS**

Tian, H; Lu, Chaoqun; Ciais, P; et al.

**JOURNAL**

Nature

**DEPOSITED IN ORE**

26 February 2016

This version available at

<http://hdl.handle.net/10871/20165>

---

**COPYRIGHT AND REUSE**

Open Research Exeter makes this work available in accordance with publisher policies.

**A NOTE ON VERSIONS**

The version presented here may differ from the published version. If citing, you are advised to consult the published version for pagination, volume/issue and date of publication

1 **The terrestrial biosphere as a net source of greenhouse gases to the atmosphere**

2  
3 Hanqin Tian<sup>1</sup>, Chaoqun Lu<sup>1,2</sup>, Philippe Ciais<sup>3</sup>, Anna M. Michalak<sup>4</sup>, Josep G. Canadell<sup>5</sup>, Eri  
4 Saikawa<sup>6</sup>, Deborah N. Huntzinger<sup>7</sup>, Kevin Gurney<sup>8</sup>, Stephen Sitch<sup>9</sup>, Bowen Zhang<sup>1</sup>, Jia  
5 Yang<sup>1</sup>, Philippe Bousquet<sup>3</sup>, Lori Bruhwiler<sup>10</sup>, Guangsheng Chen<sup>11</sup>, Edward Dlugokencky<sup>10</sup>,  
6 Pierre Friedlingstein<sup>12</sup>, Jerry Melillo<sup>13</sup>, Shufen Pan<sup>1</sup>, Benjamin Poulter<sup>14</sup>, Ronald Prinn<sup>15</sup>,  
7 Marielle Saunois<sup>3</sup>, Christopher R Schwalm<sup>7,16</sup>, Steven C. Wofsy<sup>17</sup>

[1] International Center for Climate and Global Change Research, School of Forestry and  
Wildlife Sciences, Auburn University, Auburn, AL 36849, USA

[2] Department of Ecology, Evolution, and Organismal Biology, Iowa State University, IA  
50011, USA

[3] Laboratoire des Sciences du Climat et de l'Environnement, LSCE, 91191 Gif sur Yvette,  
France

[4] Department of Global Ecology, Carnegie Institution for Science, Stanford, CA 94305, USA

[5] Global Carbon Project, CSIRO Oceans and Atmosphere, Canberra, Australia

[6] Department of Environmental Sciences, Emory University, Atlanta, GA, USA

[7] School of Earth Sciences and Environmental Sustainability, Northern Arizona University,  
Flagstaff, AZ 86011, USA

[8] School of Life Sciences, Arizona State University, Tempe, AZ 85287, USA.

[9] College of Life and Environmental Sciences, University of Exeter, Exeter, Devon, EX4 4RJ,  
UK

[10] NOAA Earth System Research Laboratory, Global Monitoring Division, Boulder Colorado,  
USA

[11] Environmental Science Division, Oak Ridge National Laboratory, Oak Ridge, TN 37831,  
USA

[12] College of Engineering, Mathematics and Physical Sciences, University of Exeter,  
EX4 4QE, UK

[13] The Ecosystem Center, Marine Biological Laboratory, Woods Hole, MA 02543, USA

[14] Department of Ecology, Montana State University, Bozeman, MT 59717, USA

[15] Center for Global Change Science, Massachusetts Institute of Technology, Cambridge, MA,  
USA

[16] Woods Hole Research Center, Falmouth MA 02540, USA

8 [17] Department of Earth and Planetary Science, Harvard University, 29 Oxford St., Cambridge,  
9 MA 02138, USA

10  
11 **Nature manuscript 2015-01-00718C**

(Accepted on 12/21/2015)

12

13 **The terrestrial biosphere can release or absorb the greenhouse gases, carbon dioxide (CO<sub>2</sub>),**  
14 **methane (CH<sub>4</sub>) and nitrous oxide (N<sub>2</sub>O) and therefore plays an important role in regulating**  
15 **atmospheric composition and climate<sup>1</sup>. Anthropogenic activities such as land use change,**  
16 **agricultural and waste management have altered terrestrial biogenic greenhouse gas fluxes**  
17 **and the resulting increases in methane and nitrous oxide emissions in particular can**  
18 **contribute to climate warming<sup>2,3</sup>. The terrestrial biogenic fluxes of individual greenhouse**  
19 **gases have been studied extensively<sup>4-6</sup>, but the net biogenic greenhouse gas balance as a**  
20 **result of anthropogenic activities and its effect on the climate system remains uncertain.**  
21 **Here we use bottom-up (BU: e.g., inventory, statistical extrapolation of local flux**  
22 **measurements, process-based modeling) and top-down (TD: atmospheric inversions)**  
23 **approaches to quantify the global net biogenic greenhouse gas balance between 1981-2010**  
24 **as a result of anthropogenic activities and its effect on the climate system. We find that the**  
25 **cumulative warming capacity of concurrent biogenic CH<sub>4</sub> and N<sub>2</sub>O emissions is about a**  
26 **factor of 2 larger than the cooling effect resulting from the global land CO<sub>2</sub> uptake in the**  
27 **2000s. This results in a net positive cumulative impact of the three GHGs on the planetary**  
28 **energy budget, with a best estimate of 3.9±3.8 Pg CO<sub>2</sub> eq/yr (TD) and 5.4±4.8 Pg CO<sub>2</sub> eq/yr**  
29 **(BU) based on the GWP 100 metric (global warming potential on a 100-year time horizon).**  
30 **Our findings suggest that a reduction in agricultural CH<sub>4</sub> and N<sub>2</sub>O emissions in particular**  
31 **in Southern Asia may help mitigate climate change.**

32 The concentration of atmospheric CO<sub>2</sub> has increased by nearly 40% since the start of the  
33 industrial era, while CH<sub>4</sub> and N<sub>2</sub>O concentrations have increased by 150% and 20%,  
34 respectively<sup>3,7,8</sup>. Although thermogenic sources (e.g., fossil fuel combustion and usage, cement  
35 production, geological and industrial processes) represent the single largest perturbation of

36 climate forcing, biogenic sources and sinks also account for a significant portion of the land-  
37 atmosphere exchange of these gases. Land biogenic GHG fluxes are those originating from  
38 plants, animals, and microbial communities, with changes driven by both natural and  
39 anthropogenic perturbations (see *Methods*). Although the biogenic fluxes of CO<sub>2</sub>, CH<sub>4</sub> and N<sub>2</sub>O  
40 have been individually measured and simulated at various spatial and temporal scales, an overall  
41 GHG balance of the terrestrial biosphere is lacking<sup>3</sup>. Simultaneous quantification of the fluxes of  
42 these three gases is needed, however, for developing effective climate change mitigation  
43 strategies<sup>9,10</sup>.

44 In the analysis that follows, we use a dual-constraint approach from 28 bottom-up (BU)  
45 studies and 13 top-down (TD) atmospheric inversion studies to constrain biogenic fluxes of the  
46 three gases. We generate decadal mean estimates and 1-sigma standard deviations of CO<sub>2</sub>, CH<sub>4</sub>  
47 and N<sub>2</sub>O fluxes (mean ± SD with SD being the square root of quadratic sum of standard  
48 deviations reported by individual studies) in land biogenic sectors by using the BU and TD  
49 ensembles as documented in *Extended Data Table 1* and *Table S2* in *Supplementary Information*  
50 (SI). Grouping GHG fluxes by sector may not precisely separate the contributions of human  
51 activities from natural components. For instance, wetland CH<sub>4</sub> emission is composed of a natural  
52 component (background emissions) and an anthropogenic contribution (e.g., emissions altered by  
53 land use and climate change). Therefore, in this study, the anthropogenic contribution to the  
54 biogenic flux of each GHG is distinguished by removing modeled pre-industrial emissions from  
55 contemporary GHG estimates. To quantify the human-induced net biogenic balance of these  
56 three GHGs and its impact on climate system, we use CO<sub>2</sub> equivalent units (CO<sub>2</sub>-eq) based on  
57 the global warming potentials (GWP) on a 100-year time horizon<sup>7</sup>. This choice has been driven  
58 by the policy options being considered when dealing with biogenic GHG emissions and sinks<sup>7,11</sup>.

59 To address the changing relative importance of each gas as a function of the selected time frame,  
60 a supplemental calculation based on GWP metrics for a 20-year time horizon is also provided  
61 (Table 1 and *Methods*).

62 We first examine the overall biogenic fluxes of all three gases in the terrestrial biosphere  
63 during the period 2000-2009 (Figure 1). The overall land biogenic CH<sub>4</sub> emissions estimated by  
64 TD and BU are very similar,  $325 \pm 39$  Tg C/yr and  $326 \pm 43$  Tg C/yr (1 Tg =  $10^{12}$  g),  
65 respectively. Among the multiple land biogenic CH<sub>4</sub> sources (*Extended Data* Table 1), natural  
66 wetlands were the largest contributor, accounting for 40-50% of total CH<sub>4</sub> emissions during the  
67 2000s, while rice cultivation contributed about 10%. The remaining CH<sub>4</sub> emissions were from  
68 ruminants (~20%), landfills and waste (~14%), biomass burning (~4-5%), manure management  
69 (~2%), and termites, wild animals and others (~6-10%). Both TD and BU results suggest a  
70 global soil CH<sub>4</sub> sink that offsets approximately 10% of global biogenic CH<sub>4</sub> emissions, but this  
71 flux is poorly constrained, especially by atmospheric inversions, given its distributed nature and  
72 small magnitude.

73 Global biogenic N<sub>2</sub>O emissions were estimated to be  $12.6 \pm 0.7$  Tg N/yr and  $15.2 \pm 1.0$   
74 Tg N/yr by TD and BU methods, respectively. Natural ecosystems were a major source,  
75 contributing ~55-60% of all land biogenic N<sub>2</sub>O emissions during the 2000s, the rest being from  
76 agricultural soils (~25-30%), biomass burning (~5%), indirect emissions (~5%), manure  
77 management (~2%), and human sewage (~2%).

78 The estimates of the global terrestrial CO<sub>2</sub> sink in the 2000s are  $-1.6 \pm 0.9$  Pg C/yr (TD)  
79 and  $-1.5 \pm 1.2$  Pg C/yr (BU). This estimate is comparable with the most recent estimates<sup>4</sup>, but  
80 incorporates more data sources (Table S1 in *SI*).

81           Some CH<sub>4</sub> and N<sub>2</sub>O emissions were present during pre-industrial times, while the global  
82 land CO<sub>2</sub> uptake was approximately in balance with the transport of carbon by rivers to the ocean  
83 and a compensatory ocean CO<sub>2</sub> source<sup>12</sup>. Thus, the net land-atmosphere CO<sub>2</sub> flux reported here  
84 represents fluxes caused by human activities. In contrast, for CH<sub>4</sub> and N<sub>2</sub>O only the difference  
85 between current and pre-industrial emissions represents net drivers of anthropogenic climate  
86 change. When subtracting modeled pre-industrial biogenic CH<sub>4</sub> and N<sub>2</sub>O emissions of 125±14  
87 TgC/yr and 7.4±1.3TgN/yr, respectively, from the contemporary estimates (see *Methods*), we  
88 find the heating capacity of human-induced land biogenic CH<sub>4</sub> and N<sub>2</sub>O emissions is opposite in  
89 sign and equivalent in magnitude to 1.7 (TD) and 2.0 (BU) times that of the current (2000s)  
90 global land CO<sub>2</sub> sink using 100-year GWPs (Figure 1, Table 1). Hence there is a net positive  
91 cumulative impact of the three GHGs on the planetary energy budget, with our “best estimate”  
92 being 3.9±3.8 Pg CO<sub>2</sub> eq/yr (TD) and 5.4±4.8 Pg CO<sub>2</sub> eq/yr (BU). An alternative GWP metric  
93 (e.g., GWP20 instead of GWP100) changes the relative importance of each gas, and gives a  
94 different view of the potential of various mitigation options<sup>11</sup>. Using GWP20 values, the  
95 radiative forcing of contemporary (2000s) human-induced biogenic CH<sub>4</sub> emission alone is 3.8  
96 (TD) or 4.2 (BU) times that of the land CO<sub>2</sub> sink in magnitude but opposite in sign, much larger  
97 than its role using GWP100 metric (Table 1). Therefore, cutting CH<sub>4</sub> emissions is an effective  
98 pathway for rapidly reducing GHG-induced radiative forcing and the rate of climate warming in  
99 a short time frame<sup>8,11</sup>.

100           On a 100-year time horizon, the cumulative radiative forcing of agricultural and waste  
101 emissions alone, including CH<sub>4</sub> from paddy fields, manure management, ruminants, and landfill  
102 and waste, along with N<sub>2</sub>O emissions from crop cultivation, manure management, human sewage  
103 and indirect emissions, are estimated to be 7.9±0.5 (BU) and 8.2±1.0 Pg CO<sub>2</sub> eq/yr (TD) for the

104 2000s, offsetting the human-induced land CO<sub>2</sub> sink by 1.4 to 1.5 times, respectively. In other  
105 words, agriculture represents the largest contributor to this twofold offset of the land CO<sub>2</sub> sink.

106 We further examine the change of human-induced biogenic GHG fluxes over past three  
107 decades (Figure 2, Table 1). The net biogenic GHG source shows a decreasing trend of 2.0 Pg  
108 CO<sub>2</sub> eq/yr per decade ( $p < 0.05$ ), primarily due to an increased CO<sub>2</sub> sink (2.2 (TD) and 2.0 (BU)  
109 Pg CO<sub>2</sub> eq/yr per decade,  $p < 0.05$ ), as driven by a combination of increasing atmospheric CO<sub>2</sub>  
110 concentrations, forest regrowth, and nitrogen deposition<sup>3</sup>. The net emissions of CO<sub>2</sub> from tropical  
111 deforestation, included in the above net land CO<sub>2</sub> sink estimates, were found to decline or remain  
112 stable due to reduced deforestation and increased forest regrowth<sup>13</sup>. However, one recent study  
113 based on satellite observations<sup>14</sup> suggests that the decreased deforestation in Brazil has been  
114 offset by an increase in deforestation in other tropical countries during 2000-2012. There is no  
115 clear decadal trend in total global biogenic CH<sub>4</sub> emissions from 1980 to 2010<sup>5</sup>. Since 2007,  
116 increased CH<sub>4</sub> emissions seem to result in a renewed and sustained increase of atmospheric CH<sub>4</sub>,  
117 although the relative contribution of anthropogenic and natural sources is still uncertain<sup>15-17</sup>. The  
118 BU estimates suggest an increase in human-induced biogenic N<sub>2</sub>O emissions since 1980, at a rate  
119 of 0.25 Pg CO<sub>2</sub> eq/yr per decade ( $p < 0.05$ ), mainly due to increasing nitrogen deposition and  
120 nitrogen fertilizer use, as well as climate warming<sup>18</sup>. With preindustrial emissions removed, the  
121 available TD estimates of N<sub>2</sub>O emissions during 1995-2008 reflect a similar positive trend,  
122 although they cover a shorter period<sup>19</sup>.

123 The human-induced biogenic GHG fluxes vary by region (Figure 3). Both TD and BU  
124 approaches indicate that human-caused biogenic fluxes of CO<sub>2</sub>, CH<sub>4</sub>, and N<sub>2</sub>O in the biosphere  
125 of Southern Asia (Figure 3) lead to a large net climate warming effect, because the 100-year  
126 cumulative effects of CH<sub>4</sub> and N<sub>2</sub>O emissions significantly exceed that of the terrestrial CO<sub>2</sub> sink.

127 Southern Asia has about 90% of global rice fields<sup>20</sup> and represents over 60% of the world's  
128 nitrogen fertilizer consumption<sup>21</sup>, with 64-81% of CH<sub>4</sub> emissions and 36-52% of N<sub>2</sub>O emissions  
129 derived from the agriculture and waste sectors (Table S3 in *SI*). Given the large footprint of  
130 agriculture in Southern Asia, improved fertilizer use efficiency, rice management and animal  
131 diets could substantially reduce global agricultural N<sub>2</sub>O and CH<sub>4</sub> emissions<sup>22,23</sup>.

132 Africa is estimated to be a small terrestrial biogenic CO<sub>2</sub> sink (BU) or a CO<sub>2</sub>-neutral  
133 region (TD), but it slightly warms the planet when accounting for human-induced biogenic  
134 emissions of CH<sub>4</sub> and N<sub>2</sub>O, which is consistent with the finding of a recent study<sup>24</sup>. South  
135 America is estimated to be neutral or a small sink of human-induced biogenic GHGs, because  
136 most current CH<sub>4</sub> and N<sub>2</sub>O emissions in this region were already present during the pre-industrial  
137 period, and therefore do not represent new emissions since the pre-industrial era. Using the  
138 GWP100 metric, CO<sub>2</sub> uptake in North America and Northern Asia is almost equivalent in  
139 magnitude or even larger than human-caused biogenic CH<sub>4</sub> and N<sub>2</sub>O emissions but opposite in  
140 sign, implying a small but significant role of the land biosphere in mitigating climate warming.  
141 Europe's land ecosystem is found to play a neutral role, similar to a previous synthesis study<sup>9</sup>  
142 using both BU and TD approaches.

143 Compared to global estimations, much more work on regional GHG budgets is  
144 needed<sup>18,19</sup>, particularly for tropical areas, as large uncertainty is revealed in both TD and BU-  
145 derived GHG estimations. TD methods are subject to large uncertainties in their regional  
146 attribution of GHG fluxes to different types of sources. Furthermore, some TD estimates used  
147 BU values as priors, and may be heavily influenced by these assumed priors in regions where  
148 atmospheric observations are sparse. In contrast, BU approaches are able to consider region-  
149 specific disturbances and drivers (e.g., insects and disease outbreaks) that are important at



150 regional scale but negligible at global scale. However, the shortcoming of BU estimates is that  
151 they may not be consistent with the well-observed global atmospheric growth rates of GHGs.  
152 Also, accurate BU assessments are hindered by our limited understanding of microbial and  
153 belowground processes and the lack of spatially-explicit, time-series datasets of drivers (e.g.,  
154 wildfire, peatland drainage, wetland extent). The magnitude of human-induced CH<sub>4</sub> and N<sub>2</sub>O  
155 emissions reported here is more uncertain than the total emissions of these gases because it  
156 contains both the uncertainty of pre-industrial emission and contemporary emission estimates  
157 (see *Methods* for additional discussion).

158         This study highlights the importance of including all three major GHGs in global and  
159 regional climate impact assessments, mitigation option and climate policy development. We  
160 should be aware of the likely countervailing impacts of mitigation efforts, such as enhanced N<sub>2</sub>O  
161 emissions with soil C sequestration<sup>25</sup>, increased CO<sub>2</sub> and N<sub>2</sub>O emissions with paddy-drying to  
162 reduce CH<sub>4</sub> emissions<sup>26</sup>, enhanced CH<sub>4</sub> emissions with peatland fire suppression and rewetting to  
163 reduce CO<sub>2</sub> and N<sub>2</sub>O emissions<sup>27</sup>, and increased indirect emissions from biofuel production<sup>28</sup>.  
164 The future role of the biosphere as a source or sink of GHGs will depend on future land use  
165 intensification pathways and on the evolution of the land CO<sub>2</sub> sinks<sup>29</sup>. If the latter continues  
166 increasing as observed in the last three decades<sup>4</sup>, the overall biospheric GHG balance could be  
167 reversed. However, the evolution of the land CO<sub>2</sub> sink remains uncertain, with some projections  
168 showing an increasing sink in the coming decades<sup>3</sup>, while others showing a weakening sink due  
169 to the saturation of the CO<sub>2</sub> fertilization effect and positive carbon-climate feedbacks<sup>3,30</sup>.  
170 Increasing land-use intensification using today's practices to meet food and energy demands will  
171 likely increase anthropogenic GHG emissions<sup>23</sup>. However, the results of this study suggest that

172 adoption of best practices to reduce GHG emissions from human-impacted land ecosystems  
173 could reverse the biosphere's current warming role.

174

## 175 **References**

176 1 Lovelock, J. E. & Margulis, L. Atmospheric homeostasis by and for the biosphere: the  
177 gaia hypothesis. *Tellus A* **26**, doi:10.3402/tellusa.v26i1-2.9731 (1974).

178 2 Vitousek, P. M., Mooney, H. A., Lubchenco, J. & Melillo, J. M. Human domination of  
179 Earth's ecosystems. *Science* **277**, 494-499 (1997).

180 3 Ciais, P., et al., Carbon and Other Biogeochemical Cycles. In: Climate Change 2013: The  
181 Physical Science Basis. Contribution of Working Group I to the Fifth Assessment Report  
182 of the Intergovernmental Panel on Climate Change [Stocker, T.F., et al.(eds.)].  
183 Cambridge University Press, Cambridge, United Kingdom and New York, NY, USA.  
184 (2013).

185 4. Le Quéré, C. *et al.* Global carbon budget 2013. *Earth System Science Data* **6**, 235-263  
186 (2014).

187 5 Kirschke, S. *et al.* Three decades of global methane sources and sinks. *Nature*  
188 *Geoscience* **6**, 813-823 (2013).

189 6 Davidson, E. A. & Kanter, D. Inventories and scenarios of nitrous oxide emissions.  
190 *Environmental Research Letters* **9**, 105012 (2014).

191 7 Myhre, G., et al., Anthropogenic and Natural Radiative Forcing Supplementary Material.  
192 In: Climate Change 2013: The Physical Science Basis. Contribution of Working Group I  
193 to the Fifth Assessment Report of the Intergovernmental Panel on Climate Change  
194 [Stocker, T.F., et al. (eds.)] (2013).

- 195 8 Montzka, S., Dlugokencky, E. & Butler, J. Non-CO<sub>2</sub> greenhouse gases and climate  
196 change. *Nature* **476**, 43-50 (2011).
- 197 9 Schulze, E. *et al.* Importance of methane and nitrous oxide for Europe's terrestrial  
198 greenhouse-gas balance. *Nature Geoscience* **2**, 842-850 (2009).
- 199 10 Tian, H. *et al.* North American terrestrial CO<sub>2</sub> uptake largely offset by CH<sub>4</sub> and N<sub>2</sub>O  
200 emissions: toward a full accounting of the greenhouse gas budget. *Climatic Change* **129**,  
201 413-426 (2014).
- 202 11 Allen, M. Short-lived promised? The Science and Policy of Cumulative and Short-Lived  
203 Climate Pollutants. *Oxford Martin Policy Paper, Oxford Martin School, University of*  
204 *Oxford* (2015).
- 205 12 Jacobson, A. R., Mikaloff Fletcher, S. E., Gruber, N., Sarmiento, J. L. & Gloor, M. A  
206 joint atmosphere-ocean inversion for surface fluxes of carbon dioxide: 1. methods and  
207 global-scale fluxes. *Global Biogeochemical Cycles* **21**, GB1019 (2007).
- 208 13 Tubiello, F. N. *et al.* The Contribution of Agriculture, Forestry and other Land Use  
209 activities to Global Warming, 1990–2012. *Global Change Biology* **21**, 2655-2660 (2015).
- 210 14 Hansen, M. C. *et al.* High-resolution global maps of 21st-century forest cover change.  
211 *Science* **342**, 850-853 (2013).
- 212 15 Dlugokencky, E. *et al.* Observational constraints on recent increases in the atmospheric  
213 CH<sub>4</sub> burden. *Geophysical Research Letters* **36**, L18803, doi:10.1029/2009GL039780  
214 (2009).
- 215 16 Rigby, M. *et al.* Renewed growth of atmospheric methane. *Geophysical Research Letters*  
216 **35**, L22805, doi:10.1029/2008GL036037(2008).

- 217 17. Nisbet, E.G., E.J. Dlugokencky and Bousquet P. Methane on the rise – again. *Science* **343**,  
218 493-494 (2014).
- 219 18 Tian, H. *et al.* Global methane and nitrous oxide emissions from terrestrial ecosystems  
220 due to multiple environmental changes. *Ecosystem Health and Sustainability* **1** (1), art4  
221 <http://dx.doi.org/10.1890/EHS14-0015.1> (2015).
- 222 19 Saikawa, E. *et al.* Global and regional emissions estimates for N<sub>2</sub>O. *Atmospheric*  
223 *Chemistry and Physics* **14**, 4617-4641 (2014).
- 224 20 Yan, X., Akiyama, H., Yagi, K. & Akimoto, H. Global estimations of the inventory and  
225 mitigation potential of methane emissions from rice cultivation conducted using the 2006  
226 Intergovernmental Panel on Climate Change Guidelines. *Global Biogeochemical Cycles*  
227 **23**, GB2002 (2009).
- 228 21 FAO. Current world fertilizer trends and outlook to 2015. (2011).
- 229 22 Smith P., et al. Agriculture, Forestry and Other Land Use (AFOLU). In: Climate Change  
230 2014: Mitigation of Climate Change. Contribution of Working Group III to the Fifth  
231 Assessment Report of the Intergovernmental Panel on Climate Change [Edenhofer, O., et  
232 al.(eds.)]. Cambridge University Press, Cambridge, United Kingdom and New York, NY,  
233 USA (2014).
- 234 23 Tilman, D., Balzer, C., Hill, J. & Befort, B. L. Global food demand and the sustainable  
235 intensification of agriculture. *Proceedings of the National Academy of Sciences* **108**,  
236 20260-20264 (2011).
- 237 24 Valentini, R. *et al.* A full greenhouse gases budget of Africa: synthesis, uncertainties, and  
238 vulnerabilities. *Biogeosciences* **11**, 381-407 (2014).

239 25 Li, C., Frolking, S. & Butterbach-Bahl, K. Carbon sequestration in arable soils is likely to  
 240 increase nitrous oxide emissions, offsetting reductions in climate radiative forcing.  
 241 *Climatic Change* **72**, 321-338 (2005).

242 26 Yu, K., Chen, G. & Patrick, W. H. Reduction of global warming potential contribution  
 243 from a rice field by irrigation, organic matter, and fertilizer management. *Global*  
 244 *Biogeochemical Cycles* **18**, GB3018 (2004).

245 27 Murdiyarso, D., Hergoualc’h, K. & Verchot, L. Opportunities for reducing greenhouse  
 246 gas emissions in tropical peatlands. *Proceedings of the National Academy of Sciences*  
 247 **107**, 19655-19660 (2010).

248 28 Melillo, J. M. *et al.* Indirect Emissions from Biofuels: How Important? *Science* **326**,  
 249 1397-1399, doi:10.1126/science.1180251 (2009).

250 29 Canadell, J. G. & Schulze, E. D. Global potential of biospheric carbon management for  
 251 climate mitigation. *Nature communications* **5**, doi:10.1038/ncomms6282 (2014).

252 30 Stocker, B. D. *et al.* Multiple greenhouse-gas feedbacks from the land biosphere under  
 253 future climate change scenarios. *Nature Climate Change* **3**, 666-672 (2013).

254

255 **Acknowledgements:** This research has been supported partially by National Aeronautics and  
 256 Space Administration (NASA) Grants (NNX08AL73G, NNX14AO73G, NNX10AU06G,  
 257 NNX11AD47G, NNG04GM39C), National Science Foundation (NSF) Grants (CNH1210360;  
 258 AGS 1243232; AGS-1243220). JGC was supported by the Australian Climate Change Science  
 259 Program. ES was supported by NOAA Climate Program Office (award # NA13OAR4310059).  
 260 CRS was supported by NASA Grants (#NNX12AP74G, #NNX10AG01A, and #NNX11AO08A).  
 261 KRG was supported by NSF CAREER (AGS-0846358). RGP was supported by NASA Upper

262 Atmosphere Research Program AGAGE Grant (NNX11AF17G to MIT). This study contributes  
263 to the Non-CO<sub>2</sub> Greenhouse Gases Synthesis of NACP (North American Carbon Program), and  
264 the Global Carbon Project (A joint project of IGBP, IHDP, WCRP and Diversitas).

265

266 **Author Contributions:** H.T. initiated this research and was responsible for the integrity of the  
267 work as a whole. H.T. and C.L. performed analysis, calculations and drafted the manuscript. P.C.,  
268 A.M. and J.C. contributed to data synthesis and manuscript development. B.Z., J.Y., G.C. and  
269 S.P. contributed to data collection and analysis. E.S., D.H., K.G., S.S., P.B., L.B., E.D., P. F.,  
270 J.M., B.P., R.P., M.S., C.S, and S.W. contributed to data provision, data processing, or  
271 interpretation. All authors discussed and commented on the manuscript.

272

273 **Figure Legends:**

274 **Figure 1. The overall biogenic greenhouse gas (GHG) balance of the terrestrial biosphere in**  
275 **the 2000s.** Top-Down (TD) and Bottom-Up (BU) approaches are used to estimate land CO<sub>2</sub> sink,  
276 CH<sub>4</sub> and N<sub>2</sub>O fluxes for four major categories merged from 14-sectors (*Extended Data Table 1*).  
277 Global warming potential (GWP 100) is calculated after removing pre-industrial biogenic  
278 emissions of CH<sub>4</sub> (125 ±14 TgC/yr) and N<sub>2</sub>O (7.4 ±1.3 Tg N/yr). Negative values indicate GHG  
279 sinks and positive values indicate GHG sources. \*TD estimates of agricultural CH<sub>4</sub> and N<sub>2</sub>O  
280 emissions include CH<sub>4</sub> source from landfill and waste, and N<sub>2</sub>O source from human sewage,  
281 respectively.

282  
283 **Figure 2. Changes in the decadal balance of human-induced biogenic greenhouse gases**  
284 **(GHG) in the past three decades (GWP 100).** TD and BU denote Top-Down and Bottom-Up  
285 estimates, respectively. Data points show individual gases (blue for CO<sub>2</sub>, yellow for CH<sub>4</sub>, and red  
286 for N<sub>2</sub>O) and human-induced GHG balance (black dots) derived from biogenic sources with pre-  
287 industrial biogenic CO<sub>2</sub> sink, and CH<sub>4</sub> and N<sub>2</sub>O emissions removed. Error bars show standard  
288 deviation calculated from various estimate ensembles.

289  
290 **Figure 3. The balance of human-induced biogenic greenhouse gases (GHG) for different**  
291 **continents in the 2000s (GWP 100).** TD and BU denote Top-Down and Bottom-Up estimates,  
292 respectively. Blue bars represent CO<sub>2</sub> flux, yellow for CH<sub>4</sub>, and red for N<sub>2</sub>O. Black dots indicate  
293 net human-induced GHG balance and error bars are standard deviation of estimate ensembles.

294  
295  
296  
297

298  
299  
300  
301

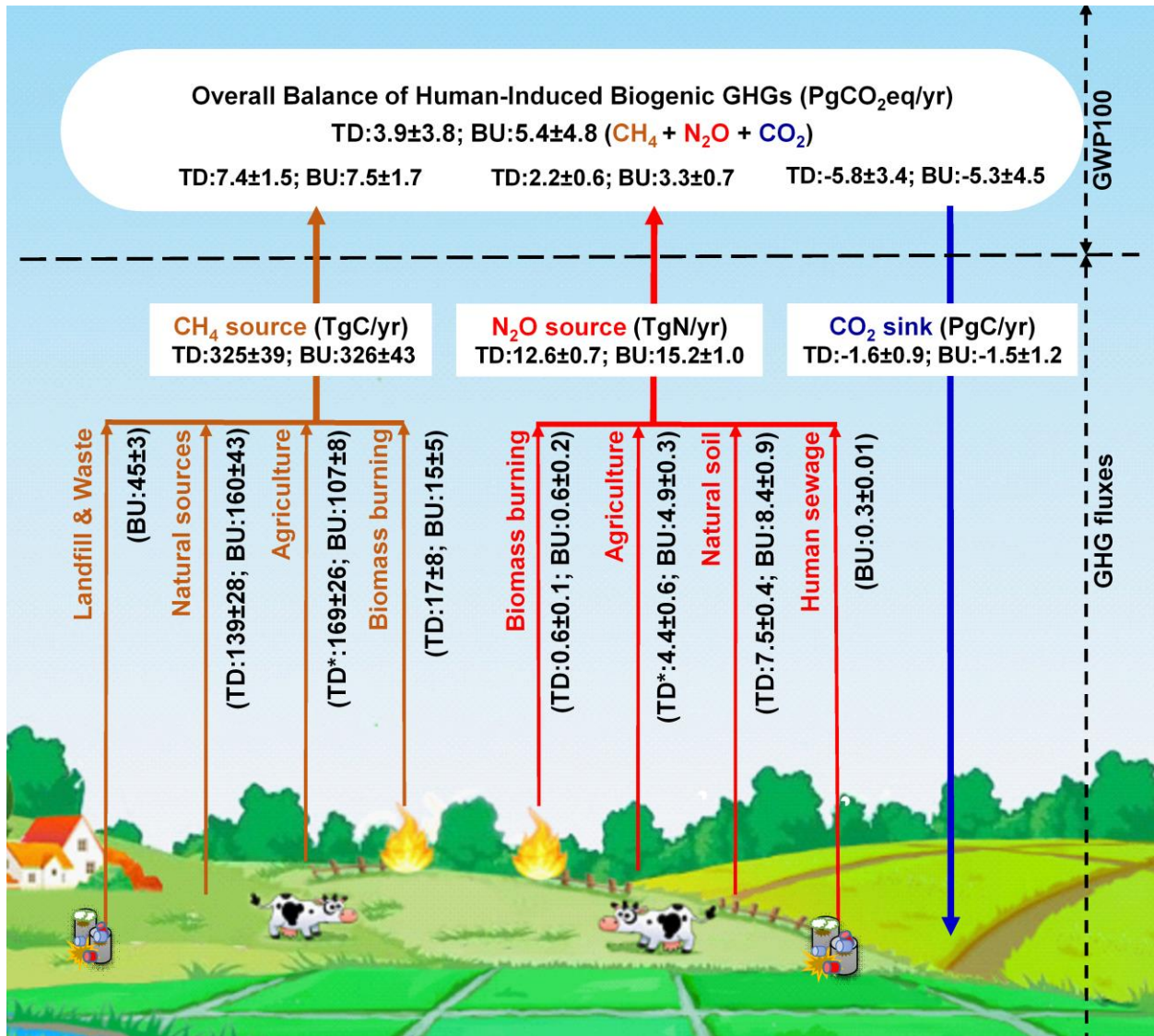
**Table 1 Three-decadal estimates of human-induced biogenic GHGs in the terrestrial biosphere by using GWP100 and GWP20 metrics.**

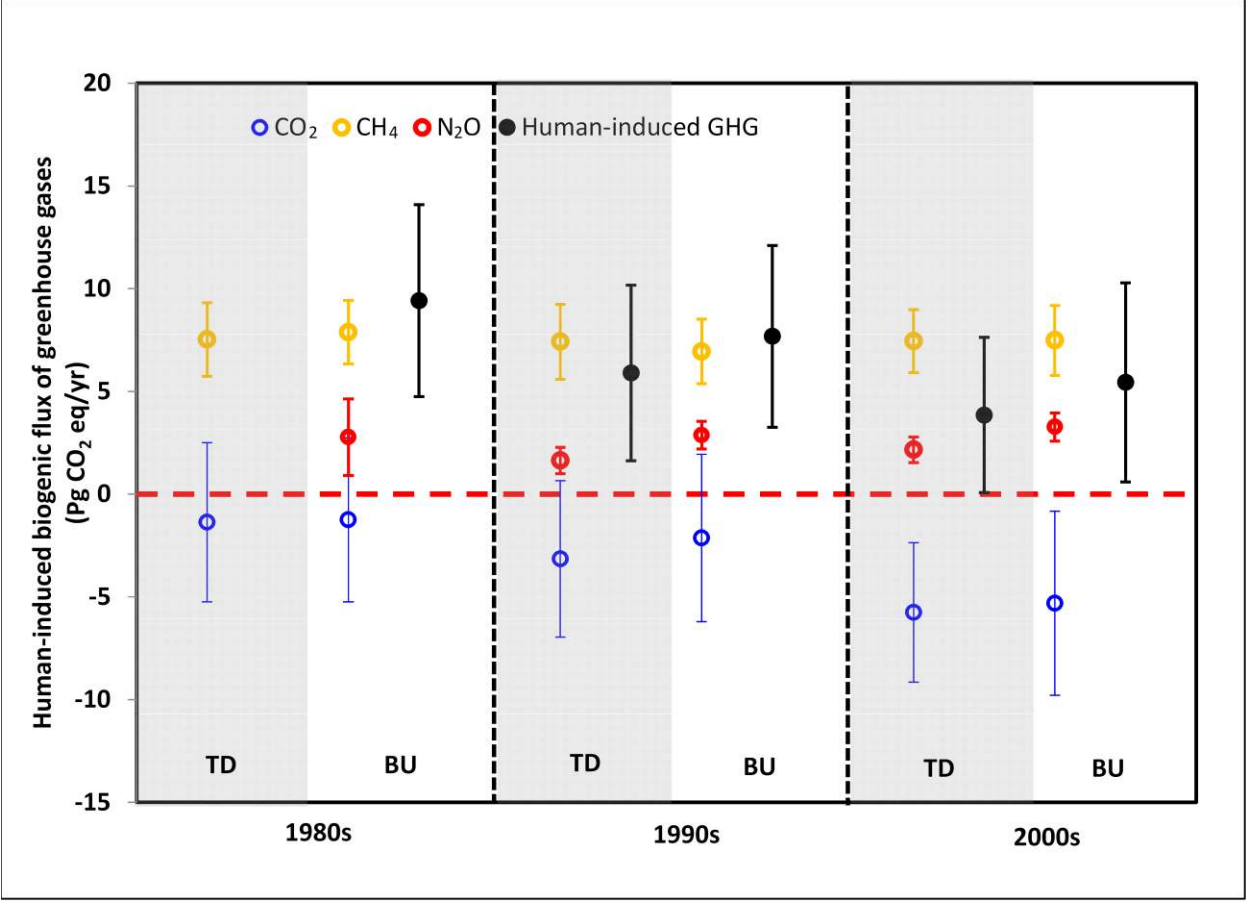
| Human-Induced GHG (Pg CO <sub>2</sub> eq/year) |  | 1980s         |               | 1990s         |               | 2000s         |               |
|--|--|---------------|---------------|---------------|---------------|---------------|---------------|
|  |  | TD            | BU            | TD            | BU            | TD            | BU            |
| GWP100   | CO <sub>2</sub> sink                                 | -1.4<br>(3.9) | -1.2<br>(4.0) | -3.2<br>(3.8) | -2.1<br>(4.1) | -5.8<br>(3.4) | -5.3<br>(4.5) |
|  | CH <sub>4</sub> source                               | 7.5<br>(1.8)  | 7.9<br>(1.5)  | 7.4<br>(1.8)  | 6.9<br>(1.6)  | 7.4<br>(1.5)  | 7.5<br>(1.7)  |
|  | N <sub>2</sub> O source                              |               | 2.8<br>(1.9)  | 1.6<br>(0.6)  | 2.9<br>(0.7)  | 2.2<br>(0.6)  | 3.3<br>(0.7)  |
|  | Overall GHG Balance                                  |               | 9.4<br>(4.7)  | 5.9<br>(4.3)  | 7.7<br>(4.4)  | 3.9<br>(3.8)  | 5.4<br>(4.8)  |
|  | Proportion of land CO <sub>2</sub> sink being offset |               | -855%         | -287%         | -460%         | -167%         | -202%         |
| GWP20  | CO <sub>2</sub> sink                                 | -1.4<br>(3.9) | -1.2<br>(4.0) | -3.2<br>(3.8) | -2.1<br>(4.1) | -5.8<br>(3.4) | -5.3<br>(4.5) |
|  | CH <sub>4</sub> source                               | 22.6<br>(5.4) | 23.6<br>(4.6) | 22.2<br>(5.5) | 20.8<br>(4.7) | 22.3<br>(4.6) | 22.5<br>(5.1) |
|  | N <sub>2</sub> O source                              |               | 2.8<br>(1.9)  | 1.6<br>(0.6)  | 2.9<br>(0.7)  | 2.2<br>(0.6)  | 3.3<br>(0.7)  |
|  | Overall GHG Balance                                  |               | 25.2<br>(6.4) | 20.7<br>(6.7) | 21.5<br>(6.3) | 18.7<br>(5.8) | 20.4<br>(6.8) |
|  | Proportion of land CO <sub>2</sub> sink being offset |               | -2118%        | -757%         | -1110%        | -425%         | -484%         |

302 Note: Estimated human-induced biogenic fluxes of CO<sub>2</sub>, CH<sub>4</sub> and N<sub>2</sub>O in the terrestrial biosphere for the  
303 1980s, 1990s, and 2000s based on global warming potential (GWP) on 20-, and 100-year time horizons.  
304 Numbers in parenthesis represent 1-sigma standard deviations. TD and BU stand for top-down and  
305 bottom-up estimates, respectively. The percentage numbers represent the proportion of land CO<sub>2</sub> sink that  
306 has been offset by human-induced CH<sub>4</sub> and N<sub>2</sub>O emissions in the terrestrial biosphere. Detailed data  
307 sources and literature cited are provided in *SI*.

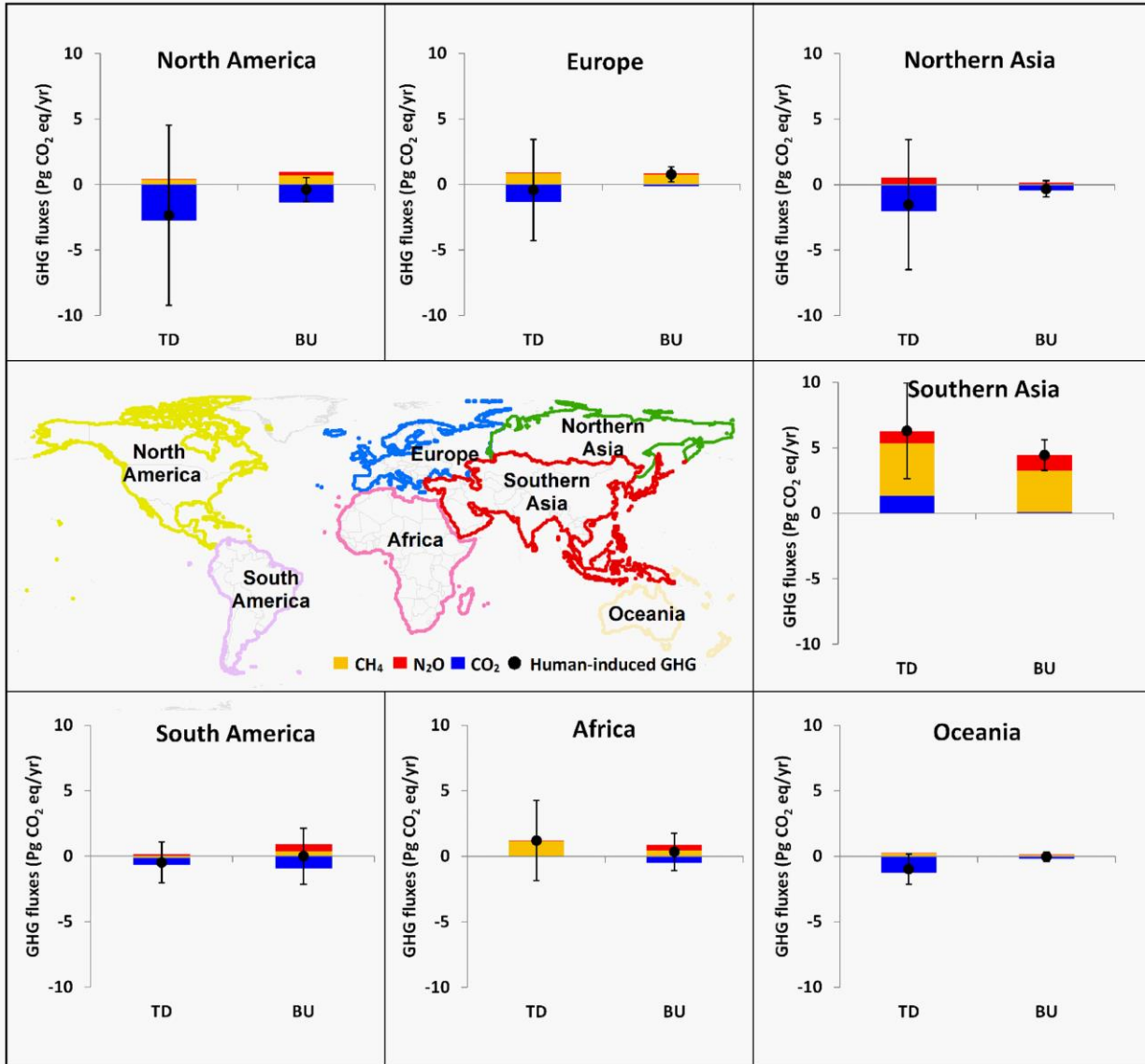
308  
309  
310







314



## 316 **Methods**

### 317 **Definition of biogenic GHG fluxes**

318 In this study, we define land biogenic GHG fluxes as those originating from plants, animals, and  
319 microbial communities, with changes driven by both natural and anthropogenic perturbations.  
320 For example, this analysis considers the biosphere-atmosphere CO<sub>2</sub> flux resulting from the direct  
321 and indirect effects of anthropogenic activities, such as land use and management, climate  
322 warming, rising atmospheric CO<sub>2</sub>, and nitrogen deposition, but excludes CO<sub>2</sub> emissions due to  
323 geological processes (e.g., volcanic eruption, weathering), fossil fuel combustion, and cement  
324 production. Biogenic CH<sub>4</sub> fluxes include land-atmosphere CH<sub>4</sub> emissions by natural wetlands,  
325 rice cultivation, biomass burning, manure management, ruminants, termites, landfills and waste,  
326 as well as soil CH<sub>4</sub> uptake. Biogenic N<sub>2</sub>O emissions include those released from agricultural  
327 ecosystems (i.e., fertilized soil emission, manure management, human sewage, and indirect N<sub>2</sub>O  
328 emission from manure and synthetic nitrogen fertilizer use), natural ecosystems (i.e., soil  
329 emissions and emissions from nitrogen re-deposition), and biomass burning.

330

### 331 **Data sources and calculation**

332 We synthesized estimates of biogenic CO<sub>2</sub>, CH<sub>4</sub> and N<sub>2</sub>O fluxes in the terrestrial biosphere  
333 derived from 28 bottom-up (BU) studies and 13 top-down (TD) atmospheric inversion studies  
334 for two spatiotemporal domains (global scale during 1981-2010 and continental scale during the  
335 2000s). The first level data sets meeting our criteria are the most recent estimates of individual  
336 GHG gases from multi-model inter-comparison projects (e.g., Atmospheric Tracer Transport  
337 Model Inter-comparison Project-TransCom<sup>31</sup>, Trends in net land atmosphere carbon exchanges –  
338 Trendy<sup>32</sup>, and Multi-scale Synthesis and Terrestrial Model Inter-comparison Project –  
339 MsTMIP<sup>33</sup>). Second, the estimate ensembles included the published global synthesis results that

340 report decadal land-atmosphere GHG exchange during 1981-2010<sup>4-6</sup>. Third, for those items that  
341 lack detailed information from the above estimations (e.g., continental estimate of CH<sub>4</sub> emission  
342 from rice fields and soil CH<sub>4</sub> sink, Table S1 in *SI*), we use multi-source published estimates and  
343 a recent process-based modeling result<sup>18</sup>. We limit literature reporting the continental GHG  
344 estimate to those studies that have close boundary delineation with our definition, and that have  
345 gas flux estimates covering all continents. Only part of global studies we used has provided  
346 continental estimates (Details on data sources can be found in Table S1 and S3 in *SI*).

347

348 In Le Quéré et al. (2014)<sup>4</sup>, net land CO<sub>2</sub> flux is the sum of carbon emission due to land use  
349 change ( $E_{LUC}$ ) and the residual terrestrial carbon sink ( $S_{LAND}$ ). Estimates of budget residual, as  
350 one of top-down approaches, are calculated as the sum of  $E_{LUC}$  and  $S_{LAND}$  (cited from Table 7 of  
351 Le Quéré et al., 2014<sup>4</sup>). Land CO<sub>2</sub> sink estimated by the TRENDY model inter-comparison  
352 project<sup>32</sup> does not account for land use effects on terrestrial carbon dynamics, and we therefore  
353 add land-use-induced carbon fluxes as estimated by IPCC AR5<sup>3</sup> (Table 6.3) to obtain the net land  
354 carbon sink estimates. However, land CO<sub>2</sub> sink estimated by MsTMIP project<sup>34</sup> is derived from  
355 model simulations considering climate variability, atmospheric CO<sub>2</sub> concentration, nitrogen  
356 deposition, as well as land use change. We directly use its model ensemble estimates in this  
357 study. In addition, BU estimates of land CO<sub>2</sub> sink<sup>4,34</sup> have been adjusted by removing the CO<sub>2</sub>  
358 emissions from drained peatland globally<sup>13,35</sup>, because global land ecosystem models usually  
359 overlook this part of carbon loss.

360

361 We include TD and BU estimates of CH<sub>4</sub> and N<sub>2</sub>O emission from biomass burning. TD approach  
362 (e.g., CarbonTracker-CH<sub>4</sub>, Bruhwiler et al., 2014<sup>36</sup>) considers all the emission sources and

363 growth rate in atmospheric concentration. For BU estimation (e.g., DLEM simulation, Tian et al.,  
364 2012<sup>37</sup>), we use historical fire data that is developed from satellite image and historical record, to  
365 drive a process-based land ecosystem model, so the change in fire occurrence is naturally  
366 considered. Other BU estimates, e.g., GFED (Van der Werf et al., 2010<sup>38</sup>) and EDGAR (2014)<sup>39</sup>  
367 all include peatland fire emissions. We remove preindustrial CH<sub>4</sub> and N<sub>2</sub>O emission that includes  
368 source from biomass burning to estimate human-caused gas fluxes in the terrestrial biosphere.  
369 The role of peatland fire in estimated CO<sub>2</sub> flux is similar to CH<sub>4</sub> and N<sub>2</sub>O estimation: fire  
370 emission is included in TD approach and historical fire is included as one of input drivers (or  
371 counted as part of land use change in most BU models, e.g., fire occurrence in deforestation and  
372 cropland expansion) in some models. Although peatland fire emission caused by human  
373 activities is counted in our analysis, like other sectors, we cannot distinguish how much peat fire  
374 is caused by human activity since no specific information is available on pre-industrial peatland  
375 fire emission.

376

377 In summary, this study provides multi-level estimates on biogenic GHG fluxes, including global  
378 biogenic fluxes of CO<sub>2</sub>, CH<sub>4</sub>, and N<sub>2</sub>O during 1981-2010, continental-level estimates on biogenic  
379 fluxes of CO<sub>2</sub>, CH<sub>4</sub> and N<sub>2</sub>O over the 2000s, and sector-based estimates on biogenic CH<sub>4</sub> and  
380 N<sub>2</sub>O fluxes over the 2000s. Extended Data Table 1 shows our estimates on biogenic CH<sub>4</sub> fluxes  
381 for 8 sectors and N<sub>2</sub>O fluxes for 6 sectors. These sectors are further merged into four major  
382 categories for CH<sub>4</sub> and N<sub>2</sub>O fluxes, respectively (Figure 1).

383

384 All the raw data and relevant calculation can be found in supplementary Table S2. Human-  
385 induced biogenic CH<sub>4</sub> and N<sub>2</sub>O emissions are calculated by subtracting the pre-industrial  
386 emissions as estimated below.

387

### 388 **Pre-industrial biogenic GHG estimations**

389 Here we provide a description of how we estimated the pre-industrial GHG emissions. For CO<sub>2</sub>  
390 flux, since terrestrial ecosystem models assume the net land-air carbon flux in the pre-industrial  
391 era is zero and the modeled C sink is solely human-driven, in order to make TD estimates  
392 comparable to BU estimates, the CO<sub>2</sub> sink from TransCom simulations<sup>31</sup> has been adjusted by  
393 removing the natural CO<sub>2</sub> sink (0.45 Pg C/yr)<sup>12</sup> due to riverine transport from land to ocean. This  
394 CO<sub>2</sub> sink of 0.45 Pg C/yr was allocated to each continent by using continental-scale estimates of  
395 riverine carbon export by Ludwig et al. (2011)<sup>40</sup> and assuming 100 Tg C/yr of organic carbon is  
396 buried and 50% of DIC export is degassing<sup>41</sup>.

397

398 Human-induced biogenic CH<sub>4</sub> and N<sub>2</sub>O emissions are calculated by subtracting the pre-industrial  
399 emissions. We define pre-industrial emissions as the GHG source under pre-industrial  
400 environmental conditions and land-use patterns, including CH<sub>4</sub> and N<sub>2</sub>O emissions from both  
401 managed (e.g., crop cultivation) and non-managed ecosystems (e.g., natural wetlands, forests,  
402 grassland, shrublands etc.). Preindustrial CH<sub>4</sub> estimate (125.4 ± 14.4 Tg C/yr) is composed of  
403 CH<sub>4</sub> emission from natural wetland and vegetation (99.2 ± 14.3 Tg C/yr derived from Houweling  
404 et al. (2008)<sup>42</sup>, Basu et al. (2014)<sup>43</sup> and unpublished result from DLEM model simulation with  
405 potential vegetation map (excluding cropland cultivation and other anthropogenic activities)),  
406 termites (15 Tg C/yr, Dlugokencky et al. (2011)<sup>44</sup>), and wildfire and wild animal (3.75-7.5 Tg

407 C/yr each, Dlugokencky et al. (2011)<sup>44</sup>). Preindustrial N<sub>2</sub>O emission (7.4 ± 1.3 Tg N/yr) is  
408 derived from the estimate of terrestrial N<sub>2</sub>O emission (6.6 ± 1.4 Tg N/yr) by Davidson and  
409 Kanter (2014)<sup>6</sup>, and DLEM simulation (8.1 ± 1.2 Tg N/yr) driven by environmental factors at  
410 preindustrial level and potential vegetation map.

411

### 412 **Calculation and interpretation of global warming potential (GWP)**

413 GWP is used to define the cumulative impacts that the emission of 1 gram CH<sub>4</sub> or N<sub>2</sub>O could  
414 have on planetary energy budget relative to 1 gram reference CO<sub>2</sub> gas over a certain period (e.g.,  
415 GWP100 and GWP20 for 100 or 20 years). To calculate CO<sub>2</sub> equivalents of the human-induced  
416 biogenic GHG balance, we adopt 100-year GWPs of 28 and 265 for CH<sub>4</sub> and N<sub>2</sub>O, respectively,  
417 and 20-year GWPs of 84 and 264, respectively<sup>7</sup>. These values of GWP 20 and 100 used in this  
418 study do not include carbon-climate feedbacks. The different contributions of each gas to the net  
419 GHG balance will vary using different GWP time horizons (e.g., GWP20 versus GWP100, see  
420 Table 1). In this study, we applied the following equation to calculate the human-induced  
421 biogenic GHG balance:

422

$$GHG = F_{CO_2-C} \frac{44}{12} + F_{CH_4-C} \frac{16}{12} \times GWP_{CH_4} + F_{N_2O-N} \frac{44}{28} \times GWP_{N_2O}$$

423

424 Where  $F_{CO_2-C}$ ,  $F_{CH_4-C}$  and  $F_{N_2O-N}$  are annual exchanges (unit: Pg C/yr or Pg N/yr) of  
425 human-induced biogenic CO<sub>2</sub>, CH<sub>4</sub> and N<sub>2</sub>O between terrestrial ecosystems and the atmosphere  
426 based on mass of C and N, respectively. The fractions  $44/12$ ,  $16/12$  and  $44/28$  were used to  
427 convert the mass of CO<sub>2</sub>-C, CH<sub>4</sub>-C and N<sub>2</sub>O-N into CO<sub>2</sub>, CH<sub>4</sub> and N<sub>2</sub>O.  $GWP_{CH_4}$  (Pg CO<sub>2</sub> eq/Pg



428 CH<sub>4</sub>) and  $GWP_{N_2O}$  (Pg CO<sub>2</sub> eq/Pg N<sub>2</sub>O) are constants indicating integrated radiative forcing of  
429 CH<sub>4</sub> and N<sub>2</sub>O in terms of a CO<sub>2</sub> equivalent unit.  
430  
431 Nevertheless, it is noted that adoption of GWP100 to calculate CO<sub>2</sub> equivalent is not  
432 fundamentally scientific but depends on a policy perspective. The relative importance of each  
433 gas at a certain time period and likely mitigation option could change due to GWP metrics at  
434 different time horizon (e.g., GWP20 and GWP100 according to Myhre et al., 2013<sup>7</sup>, Table 1).  
435 For example, CH<sub>4</sub> has a shorter lifetime (~9 years), and its cumulative radiative forcing is  
436 equivalent to 84 times same amount of CO<sub>2</sub> over 20 years, and 28 times same amount of CO<sub>2</sub>  
437 over 100 years. At a 20-year time horizon, anthropogenic CH<sub>4</sub> and N<sub>2</sub>O emissions in the 2000s  
438 are equivalent to 4.2-4.8 (TD-BU) times land CO<sub>2</sub> sink in magnitude but opposite in sign, and  
439 net balance of human-induced GHG in the terrestrial biosphere is  $20.4 \pm 6.8$  Pg CO<sub>2</sub> eq/yr and  
440  $18.7 \pm 5.8$  Pg CO<sub>2</sub> eq/yr as estimated by BU and TD approaches, respectively. Among them,  
441 anthropogenic CH<sub>4</sub> emissions are 7-10 times (BU-TD) as much as N<sub>2</sub>O emissions in terms of  
442 GWP20. At a 20-year time horizon, the cumulative radiative forcing of contemporary  
443 anthropogenic CH<sub>4</sub> emission alone is 3.8-4.2 (TD-BU) times as much as that of land CO<sub>2</sub> sink  
444 but opposite in sign, larger than its role at 100-year time horizon (1.3-1.4 times radiative forcing  
445 of CO<sub>2</sub> sink). Therefore, to cut CH<sub>4</sub> emission could rapidly reduce GHG-induced radiative  
446 forcing in a short time frame<sup>7,8,44</sup>.

447

#### 448 **Statistics**

449 We use mean  $\pm$  1-sigma standard deviations (SD) to indicate the best estimates and their ranges.  
450 Estimate ensembles are grouped for the TD and BU approaches, and the mean value of multiple

451 ensembles is calculated for each gas in a certain region and period. In the TD and BU groups, we  
452 assume the individual estimates are independent from each other, and therefore, the SD for each  
453 ensemble mean is calculated as the square root of the quadratic sum of standard deviations  
454 reported in each estimate.

455

### 456 **Continental-level estimations and divergence of biogenic-GHG fluxes**

457 Using the TD and BU ensembles, we estimated the net human-induced biogenic GHG balance  
458 during the 2000s for 7 continents or regions, which include North America, South America,  
459 Europe, Northern Asia, Southern Asia, Africa and Oceania (Figure 1). Primarily owing to large  
460 CH<sub>4</sub> and N<sub>2</sub>O emissions, both approaches show that Southern Asia is a net human-induced  
461 biogenic GHG source in the magnitude of  $6.3 \pm 3.7$  and  $4.4 \pm 1.2$  Pg CO<sub>2</sub> eq/yr as estimated by  
462 TD and BU, respectively, with the GWP100 metric (Table S3). Southern Asia has about 90% of  
463 the global rice fields and represents over 60% of the world's nitrogen fertilizer consumption.  
464 China and India together consume half of global nitrogen fertilizer<sup>21</sup>. This leads to the highest  
465 regional CH<sub>4</sub> and N<sub>2</sub>O emissions as the two approaches consistently reveal. This finding is also  
466 consistent with previous studies conducted in China and India<sup>45-47</sup>. South America was estimated  
467 to be a CO<sub>2</sub> sink with a large uncertainty (Table S3). Although South America is a large CH<sub>4</sub> and  
468 N<sub>2</sub>O source, most of these emissions are present at pre-industrial times. Natural wetlands in  
469 South America accounted for 31-40% of global wetland CH<sub>4</sub> emissions in the 2000s, and 26-30%  
470 of the global natural soil N<sub>2</sub>O emissions were derived from this region. Therefore, the  
471 contribution of this continent to human-induced GHG balance is negligible or acts as a small  
472 sink. Likewise, Africa is estimated to be a small CO<sub>2</sub> sink or CO<sub>2</sub>-neutral region, but adding CH<sub>4</sub>

473 and N<sub>2</sub>O emissions makes this continent contribute a small positive radiative forcing, slightly  
474 warming the planet.  
475  
476 North America and Northern Asia are found to be a neutral region to net human-induced  
477 biogenic GHG sink, with 100-year cumulative radiative forcing of biogenic CH<sub>4</sub> and N<sub>2</sub>O  
478 emissions fully or partially offsetting that of land CO<sub>2</sub> sink in this continent (Table S3). The  
479 largest CO<sub>2</sub> sink was found in North America, ranging from  $-0.37 \pm 0.22$  to  $-0.75 \pm 1.87$  Pg C/yr  
480 as estimated by TD and BU, respectively, likely due to larger area of highly productive and  
481 intensively managed ecosystems (e.g., forests, woodlands, and pasture) that were capable of  
482 sequestering more CO<sub>2</sub>. Our estimate falls within the newly-reported CO<sub>2</sub> sink of  $-0.28$  to  $-0.89$   
483 Pg C/yr in North America by synthesizing inventory, atmospheric inversions, and terrestrial  
484 modeling estimates<sup>48</sup>. Considering three gases together, TD estimates showed that the North  
485 America acts as a net GHG sink with a large standard deviation (human-induced biogenic GHG  
486 of  $-2.35 \pm 6.87$  Pg CO<sub>2</sub> eq/yr, Figure 3 and Table S3). By contrast, BU estimates suggested that  
487 North America was a small GHG sink, in the magnitude of  $-0.38 \pm 0.93$  Pg CO<sub>2</sub> eq/yr based on  
488 GWP100. Our estimate is comparable to previous GHG budget syntheses for North America<sup>10,37</sup>.  
489 TD estimates indicated that Oceania and Europe act as a small negative net radiative forcing over  
490 100 years ( $-0.98 \pm 1.17$  and  $-0.42 \pm 3.86$  Pg CO<sub>2</sub> eq/yr, respectively), while BU estimates  
491 indicated a negligible contribution in Oceania, and a positive net radiative forcing ( $0.76 \pm 0.57$   
492 Pg CO<sub>2</sub> eq/yr) in Europe. According to BU estimates, CO<sub>2</sub> emission from drained peatland in  
493 Europe accounted for about one third of global total during the period 2000s<sup>35</sup>, which partially  
494 explains the warming effect of biogenic GHG in this region as revealed by BU.  
495

496

497 It is important to note that only human-caused biogenic GHG fluxes are included in this study,  
498 and the regional GHG balance will clearly move towards a net source if the emissions related to  
499 fossil fuel combustion and usage are taken into account.

500

501 Our analyses indicate that the TD and BU estimates show a larger divergence at continental scale  
502 than global scale. We notice that the high radiative forcing estimate of human-induced biogenic  
503 GHG balance ( $6.30 \pm 3.66$  Pg CO<sub>2</sub> eq/yr) in the TD approach in Southern Asia is partially  
504 because the land biosphere in this region is estimated to be a net CO<sub>2</sub> source of 0.36 Pg C/yr with  
505 a large standard deviation of 0.99 Pg C/yr by TransCom Inversions<sup>31,49</sup>. It includes CO<sub>2</sub> sources  
506 and sinks from respiration, primary production, disturbances, rivers outgassing, and land use  
507 change. In contrast, most BU estimations using land ecosystem models do not consider the full  
508 set of factors responsible for CO<sub>2</sub> release<sup>32,33</sup>. The discrepancy between TD and BU estimates for  
509 Southern Asia may come from several reasons. First, the land use history data commonly used  
510 for driving terrestrial biosphere models, e.g., HYDE<sup>50</sup> and GLM<sup>51</sup>, was reported to overestimate  
511 cropland area and cropland expansion rate in China and to under-estimate it in India compared to  
512 regional dataset<sup>52,53</sup>, thus biasing BU estimates of land conversion-induced carbon fluxes. But  
513 none of BU models included in this study conducted global simulation with such regional dataset  
514 updated. Second, large uncertainties exist in estimating carbon release due to tropical  
515 deforestation<sup>4,54-57</sup>. Third, carbon emissions due to peat fires and peatland drainage were a large  
516 but usually ignored carbon source in tropical Asia (EDGAR 4.2<sup>39</sup> and Joosten et al., 2010<sup>35</sup>). In  
517 the BU estimates we included, some models consider peat fire by using input driver of fire  
518 regime from satellite images, while most of them don't consider drained peatland and accelerated

519 SOC decomposition. Therefore, BU models may underestimate the CO<sub>2</sub> emissions at intensively-  
520 disturbed areas, resulting in a small CO<sub>2</sub> source of  $0.03 \pm 0.29$  Pg C/yr. BU estimations show  
521 that the net human-induced biogenic GHG balance in Southern Asia turned out to warm the  
522 planet with the 100-year cumulative radiative forcing of  $4.44 \pm 1.17$  Pg CO<sub>2</sub> eq/yr.

523

524 Net GHG balance in Africa was positive but with discrepancy between the TD and BU  
525 approaches. TD estimates suggest that Africa was a weak source of CO<sub>2</sub> and a strong source of  
526 CH<sub>4</sub> and N<sub>2</sub>O, resulting in a positive net radiative forcing of  $1.20 \pm 3.05$  Pg CO<sub>2</sub> eq/yr. However,  
527 BU ensembles estimate that African terrestrial biosphere acted as a relatively smaller climate  
528 warmer ( $0.34 \pm 1.42$  Pg CO<sub>2</sub> eq/yr) due to an anthropogenic land sink of CO<sub>2</sub> ( $-0.52 \pm 1.38$  Pg  
529 CO<sub>2</sub> eq/yr) and a strong source of CH<sub>4</sub> and N<sub>2</sub>O. The divergent estimates in Africa might have  
530 several reasons. First, it was difficult to constrain emissions using TD in this region, due to the  
531 lack of atmospheric data. No tropical continent is covered by enough atmospheric GHG  
532 measurement stations, making the TD results uncertain in those regions, with almost no  
533 uncertainty reduction from the prior knowledge assumed before inversion. Second, there were  
534 also large uncertainties in BU estimates. Some of the BU models ignored fire disturbance that is  
535 likely to result in a carbon source of  $1.03 \pm 0.22$  Pg C/yr in Africa<sup>24,38</sup> and this emission has been  
536 partially offset by carbon uptake due to regrowth. Another reason might be the overestimated  
537 CO<sub>2</sub> fertilization effect, which could be limited by nutrient availability. Only few BU models  
538 addressed interactive nutrient cycles in their simulation experiments<sup>32</sup>.

539

540 **Uncertainty sources and future research needs**

541 A wide variety of methods, such as statistical extrapolations, and process-based and inverse  
542 modeling, were applied to estimate CO<sub>2</sub>, CH<sub>4</sub> and N<sub>2</sub>O fluxes. TD methods are subject to large  
543 uncertainties in their regional attribution of GHG fluxes to different type of sources<sup>58</sup>. BU  
544 approaches are however limited by our understanding of underlying mechanisms and the  
545 availability and quality of input data. In addition, the TD approach is dependent on BU estimates  
546 as prior knowledge, especially in the tropics where both uncertainties are very large.

547

548 For example, terrestrial CO<sub>2</sub> uptake estimates from process-based model ensembles in Africa,  
549 South America, and Southern Asia are larger than those from TD approaches, while smaller than  
550 TD estimates in North America, Europe, Oceania and Northern Asia (Figure 3, Table S3). The  
551 larger BU CO<sub>2</sub> sink estimate might be related to biased land use history data, excluded fire  
552 emission and CO<sub>2</sub> release due to extreme disturbances such as insect outbreaks and  
553 windthrow<sup>24,32</sup>. Another reason is the lack of fully-coupled carbon-nitrogen-phosphorous cycles  
554 in most BU models that overestimate the CO<sub>2</sub> fertilization effect particularly in regions of large  
555 biomass and large productivity<sup>59-61</sup>. However, larger CO<sub>2</sub> sink observed from tropical regrowth  
556 forests compared to intact forests<sup>55</sup> might be underestimated because few models are capable of  
557 capturing CO<sub>2</sub> uptake related to tropical secondary forest management and age structure. The  
558 post-disturbance and plantation-induced shift toward rapid carbon accumulation in young forests  
559 that were poorly or not represented in terrestrial ecosystem models might be one of the factors  
560 responsible for CO<sub>2</sub> sink underestimation as revealed by several studies conducted in mid- and  
561 high-latitudes<sup>62-64</sup>. The modeled ecosystem responses to frequent occurrence of extreme climate  
562 events in BU studies are another uncertainty in estimating variations of land CO<sub>2</sub> sink<sup>65,66</sup>.

563

564 The estimates of terrestrial CH<sub>4</sub> fluxes remain largely uncertain. One major uncertainty in BU  
565 wetland CH<sub>4</sub> emission estimate is wetland areal extent data<sup>67</sup>. Global inundated area extent was  
566 reported to decline by approximately 6% during 1993-2007 with the largest decrease in tropical  
567 and subtropical South America and South Asia<sup>68</sup>. However, the majority of BU models failed  
568 either in capturing dynamic inundation area or in simulating inundation and saturated conditions.  
569 Tropical emissions, the dominant contributor for global wetland emission, are particularly  
570 difficult to quantify due to sparse observations for both TD (atmospheric mixing ratios) and BU  
571 (flux measurements) approaches and large interannual, seasonal variability, and long-term  
572 change in the inundation extent for the BU modeling approach<sup>5,36,68</sup>. At high latitudes, current  
573 dynamic inundation data could not well represent permanent wetlands<sup>67</sup>, most of which are  
574 occupied by peatland. Due to large soil carbon storage in peatlands, such area is an important  
575 CH<sub>4</sub> source. In addition, a large divergence exists in the estimation of rice field CH<sub>4</sub> emissions  
576 (Table S2). The estimated global CH<sub>4</sub> emissions from rice fields are sensitive to rice field area,  
577 management practices (e.g., water regime, nutrient fertilizer), and local climate and soil  
578 conditions that directly affect activities of methanotroph and methanogen<sup>20,69,70</sup>. Models need  
579 better representation of CH<sub>4</sub> production and consumption processes modified by agricultural  
580 management, such as continuous flooding, irrigation with intermediate drainage, or rainfed<sup>70</sup>.  
581  
582 Compared to CO<sub>2</sub> and CH<sub>4</sub>, there were fewer studies for global N<sub>2</sub>O emissions. The TD  
583 approach is constrained by sparse or inconsistent measurements of atmospheric N<sub>2</sub>O mixing  
584 ratios<sup>19,71</sup>. Decadal trends during 1981-2010 from BU approaches were primarily from two  
585 process-based models<sup>18,72</sup>, instead of IPCC methodology based on the N<sub>2</sub>O emission factors. The  
586 major uncertainty source, therefore, includes data characterizing spatiotemporal variation of

587 reactive nitrogen enrichment, modeling schemes representing multiple nitrogen forms,  
588 transformation, and their interactions with other biogeochemical and hydrological cycles, as well  
589 as key parameters determining the sensitivity of N<sub>2</sub>O emission to temperature, soil moisture, and  
590 availability of oxygen<sup>45,46,72-74</sup>. A large divergence exists in the estimation of natural soil N<sub>2</sub>O  
591 emission by inventory, empirical and process-based models, implying that our understanding of  
592 the processes and their controls remain uncertain<sup>18,72,75-77</sup>. Tropical areas are the major  
593 contributors to large divergence. N<sub>2</sub>O sources from tropical undisturbed wetland and drained  
594 wetland/peatland are likely to be underestimated<sup>78</sup>.

595

596 31 Gurney, K. R., Baker, D., Rayner, P. & Denning, S. Interannual variations in continental-  
597 scale net carbon exchange and sensitivity to observing networks estimated from  
598 atmospheric CO<sub>2</sub> inversions for the period 1980 to 2005. *Global biogeochemical cycles*  
599 **22**, GB3025 (2008).

600 32 Sitch, S. *et al.* Recent trends and drivers of regional sources and sinks of carbon dioxide.  
601 *Biogeosciences* **12**, 653-679 (2015).

602 33 Huntzinger, D. *et al.* The north american carbon program multi-scale synthesis and  
603 terrestrial model intercomparison project–part 1: Overview and experimental design.  
604 *Geoscientific Model Development* **6**, 2121-2133 (2013).

605 34 Schwalm, C. R. *et al.* Toward “optimal” integration of terrestrial biosphere models.  
606 *Geophysical Research Letters*, 4418-4428 (2015).

607 35 Joosten, H., The Global Peatland CO<sub>2</sub> Picture Peatland status and drainage related  
608 emissions in all countries of the world. Greifswald University Wetlands International,  
609 Ede, August 2010 [www.wetlands.org](http://www.wetlands.org).



610 36 Bruhwiler, L. *et al.* CarbonTracker-CH<sub>4</sub>: an assimilation system for estimating emissions  
611 of atmospheric methane. *Atmospheric Chemistry and Physics* **14**, 8269-8293 (2014).

612 37 Tian, H. *et al.* Contemporary and projected biogenic fluxes of methane and nitrous oxide  
613 in North American terrestrial ecosystems. *Frontiers in Ecology and the Environment* **10**,  
614 528-536 (2012).

615 38 van der Werf, G. R. *et al.* Global fire emissions and the contribution of deforestation,  
616 savanna, forest, agricultural, and peat fires (1997–2009). *Atmospheric Chemistry and*  
617 *Physics* **10**, 11707-11735 (2010).

618 39 EDGAR. Emission Database for Global Atmospheric Research (EDGAR) release version  
619 4.2. (2014).

620 40 Ludwig, W., Amiotte-Suchet, P. & Probst, J. ISLSCP II atmospheric carbon dioxide  
621 consumption by continental erosion. doi:10.3334/ORNLDAAAC/1019 (2011).

622 41 Sarmiento, J. & Sundquist, E. Revised budget for the oceanic uptake of anthropogenic  
623 carbon dioxide. *Nature* **356**, 589-593 (1992).

624 42 Houweling, S., Van der Werf, G., Klein Goldewijk, K., Röckmann, T. & Aben, I. Early  
625 anthropogenic CH<sub>4</sub> emissions and the variation of CH<sub>4</sub> and <sup>13</sup>CH<sub>4</sub> over the last  
626 millennium. *Global Biogeochemical Cycles* **22**, GB1002 (2008).

627 43 Basu, A. *et al.* Analysis of the global atmospheric methane budget using ECHAM-MOZ  
628 simulations for present-day, pre-industrial time and the Last Glacial Maximum. *Atmos.*  
629 *Chem. Phys. Discuss.* **14**, 3193-3230 (2014).

630 44 Dlugokencky, E. J., Nisbet, E. G., Fisher, R. & Lowry, D. Global atmospheric methane:  
631 budget, changes and dangers. *Philosophical Transactions of the Royal Society A:*  
632 *Mathematical, Physical and Engineering Sciences* **369**, 2058-2072 (2011).

- 633 45 Lu, C. & Tian, H. Net greenhouse gas balance in response to nitrogen enrichment:  
634 perspectives from a coupled biogeochemical model. *Global change biology* **19**, 571-588  
635 (2013).
- 636 46 Tian, H. *et al.* Net exchanges of CO<sub>2</sub>, CH<sub>4</sub>, and N<sub>2</sub>O between China's terrestrial  
637 ecosystems and the atmosphere and their contributions to global climate warming.  
638 *Journal of Geophysical Research: Biogeosciences* **116**, doi:10.1029/2010JG001393  
639 (2011).
- 640 47 Banger, K. *et al.* Biosphere–atmosphere exchange of methane in India as influenced by  
641 multiple environmental changes during 1901–2010. *Atmospheric Environment* **119**, 192-  
642 200 (2015).
- 643 48 King, A. *et al.* North America's net terrestrial CO<sub>2</sub> exchange with the atmosphere 1990–  
644 2009. *Biogeosciences* **12**, 399-414 (2015).
- 645 49 Baker, D. *et al.* TransCom 3 inversion intercomparison: Impact of transport model errors  
646 on the interannual variability of regional CO<sub>2</sub> fluxes, 1988–2003. *Global Biogeochemical*  
647 *Cycles* **20** (2006).
- 648 50 Goldewijk, K. K. Estimating global land use change over the past 300 years: the HYDE  
649 database. *Global Biogeochemical Cycles* **15**, 417-433 (2001).
- 650 51 Hurtt, G. *et al.* The underpinnings of land-use history: Three centuries of global gridded  
651 land-use transitions, wood-harvest activity, and resulting secondary lands. *Global Change*  
652 *Biology* **12**, 1208-1229 (2006).
- 653 52 Liu, M. & Tian, H. China's land cover and land use change from 1700 to 2005:  
654 Estimations from high-resolution satellite data and historical archives. *Global*  
655 *Biogeochemical Cycles* **24**, GB3003 (2010).

656 53 Tian, H., Banger, K., Bo, T. & Dadhwal, V. K. History of land use in India during 1880–  
657 2010: Large-scale land transformations reconstructed from satellite data and historical  
658 archives. *Global and Planetary Change* **121**, 78-88 (2014).

659 54 Friedlingstein, P. *et al.* Update on CO<sub>2</sub> emissions. *Nature Geoscience* **3**, 811-812 (2010).

660 55 Pan, Y. *et al.* A large and persistent carbon sink in the world's forests. *Science* **333**, 988-  
661 993 (2011).

662 56 Harris, N. L. *et al.* Baseline map of carbon emissions from deforestation in tropical  
663 regions. *Science* **336**, 1573-1576 (2012).

664 57 Archer-Nicholls, S. *et al.* Characterising Brazilian biomass burning emissions using  
665 WRF-Chem with MOSAIC sectional aerosol. *Geoscientific Model Development* **8**, 549-  
666 577 (2015).

667 58 Peylin, P. *et al.* Global atmospheric carbon budget: results from an ensemble of  
668 atmospheric CO<sub>2</sub> inversions. *Biogeosciences* **10**, 6699-6720 (2013).

669 59 Thornton, P. E. *et al.* Carbon-nitrogen interactions regulate climate-carbon cycle  
670 feedbacks: results from an atmosphere-ocean general circulation model. *Biogeosciences* **6**,  
671 2099-2120 (2009).

672 60 Sokolov, A. P. *et al.* Consequences of considering carbon-nitrogen interactions on the  
673 feedbacks between climate and the terrestrial carbon cycle. *Journal of Climate* **21**, 3776-  
674 3796 (2008).

675 61 Zaehle, S., Friedlingstein, P. & Friend, A. D. Terrestrial nitrogen feedbacks may  
676 accelerate future climate change. *Geophysical Research Letters* **37**, L01401 (2010).

677 62 Goward, S. N. *et al.* Forest disturbance and North American carbon flux. *Eos*,  
678 *Transactions American Geophysical Union* **89**, 105-106 (2008).

679 63 Williams, C. A., Collatz, G. J., Masek, J. & Goward, S. N. Carbon consequences of forest  
680 disturbance and recovery across the conterminous United States. *Global Biogeochemical*  
681 *Cycles* **26**, GB1005 (2012).

682 64 Bellassen, V. *et al.* Reconstruction and attribution of the carbon sink of European forests  
683 between 1950 and 2000. *Global Change Biology* **17**, 3274-3292 (2011).

684 65 Reichstein, M. *et al.* Climate extremes and the carbon cycle. *Nature* **500**, 287-295 (2013).

685 66 Zscheischler, J. *et al.* Impact of large-scale climate extremes on biospheric carbon fluxes:  
686 An intercomparison based on MsTMIP data. *Global Biogeochemical Cycles* **28**, 585-600  
687 (2014).

688 67 Melton, J. *et al.* Present state of global wetland extent and wetland methane modelling:  
689 conclusions from a model intercomparison project (WETCHIMP). *Biogeosciences* **10**,  
690 753-788 (2013).

691 68 Prigent, C. *et al.* Changes in land surface water dynamics since the 1990s and relation to  
692 population pressure. *Geophysical Research Letters* **39**, L08403 (2012).

693 69 Ren, W. *et al.* Spatial and temporal patterns of CO<sub>2</sub> and CH<sub>4</sub> fluxes in China's croplands  
694 in response to multifactor environmental changes. *Tellus B* **63**, 222-240 (2011).

695 70 Banger, K., Tian, H. & Lu, C. Do nitrogen fertilizers stimulate or inhibit methane  
696 emissions from rice fields? *Global Change Biology* **18**, 3259-3267 (2012).

697 71 Reay, D. S. *et al.* Global agriculture and nitrous oxide emissions. *Nature Climate Change*  
698 **2**, 410-416 (2012).

699 72 Saikawa, E., Schlosser, C. & Prinn, R. Global modeling of soil nitrous oxide emissions  
700 from natural processes. *Global Biogeochemical Cycles* **27**, 972-989 (2013).

701 73 Bouwman, A. *et al.* Global trends and uncertainties in terrestrial denitrification and N<sub>2</sub>O  
702 emissions. *Philosophical Transactions of the Royal Society B: Biological Sciences* **368**,  
703 (2013).

704 74 Butterbach-Bahl, K., Diaz-Pines, E. & Dannenmann, M. Soil trace gas emissions and  
705 climate change. *Global Environmental Change* 325-334 (Springer, 2014).

706 75 Potter, C. S., Matson, P. A., Vitousek, P. M. & Davidson, E. A. Process modeling of  
707 controls on nitrogen trace gas emissions from soils worldwide. *Journal of Geophysical*  
708 *Research: Atmospheres (1984–2012)* **101**, 1361-1377 (1996).

709 76 Xu, X., Tian, H. & Hui, D. Convergence in the relationship of CO<sub>2</sub> and N<sub>2</sub>O exchanges  
710 between soil and atmosphere within terrestrial ecosystems. *Global change biology* **14**,  
711 1651-1660 (2008).

712 77 Zhuang, Q. *et al.* Response of global soil consumption of atmospheric methane to  
713 changes in atmospheric climate and nitrogen deposition. *Global Biogeochemical Cycles*  
714 **27**, 650-663 (2013).

715 78 Liengaard, L. *et al.* Extreme emission of N<sub>2</sub>O from tropical wetland soil (Pantanal, South  
716 America). *Frontiers in microbiology* **3** (2012).

717  
718  
719

Extended Data Table 1 | Decadal estimates of global terrestrial CO<sub>2</sub>, CH<sub>4</sub> and N<sub>2</sub>O fluxes derived from Top-Down and Bottom-Up approaches

| GHG                           | Sector  | 1980s             |                   | 1990s             |                   | 2000s             |                   |
|-------------------------------|---|-------------------|-------------------|-------------------|-------------------|-------------------|-------------------|
|                               |   | Top-down          | Bottom-up         | Top-down          | Bottom-up         | Top-down          | Bottom-up         |
| CO <sub>2</sub><br>(Pg C/yr)  | <b>Net land CO<sub>2</sub> sink</b>           | <b>-0.4±1.1</b>   | <b>-0.3±1.1</b>   | <b>-0.9±1.0</b>   | <b>-0.6±1.1</b>   | <b>-1.6±0.9</b>   | <b>-1.5±1.2</b>   |
|                               | 1) Natural wetland                            | 125.3±43.5        | 168.8±31.1        | 112.5±6.0         | 154.5±36.0        | 131.3±24.8        | 162.8±40.1        |
|                               | 2) Soil sinks                                 | -15.8±6.4         | -19.7±14.3        | -20.3±0.0         | -21.5±14.3        | -24.0±6.0         | -22.6±14.3        |
|                               | 3) Termite, Wild animal & Others              | 27.0±0.4          | 19.5±3.8          | 24.0±5.3          | 19.5±3.8          | 32.3±10.5         | 19.5±3.8          |
|                               | <b>Natural*</b>                               | <b>136.5±44.0</b> | <b>168.6±34.5</b> | <b>116.3±8.0</b>  | <b>152.5±38.9</b> | <b>138.8±27.6</b> | <b>159.6±42.8</b> |
|                               | <b>4) Biomass burning</b>                     | <b>34.5±2.3</b>   | <b>16.3±5.7</b>   | <b>28.5±3.6</b>   | <b>19.1±7.9</b>   | <b>17.3±7.9</b>   | <b>14.8±5.4</b>   |
|                               | 5) Rice cultivation                           |                   | 45.4±16.8         | 86.3±21.0         | 26.3±5.6          | 33.0±2.0          | 28.9±7.6          |
|                               | 6) Manure management                          |                   | 7.8±0.2           |                   | 7.9±0.1           |                   | 8.0±0.3           |
|                               | 7) Ruminant                                   |                   | 64.8±2.2          |                   | 66.0±0.9          |                   | 70.0±3.3          |
|                               | 8) Landfill and Waste                         |                   | 33.6±2.3          |                   | 39.5±2.0          |                   | 44.7±3.3          |
| CH <sub>4</sub><br>(Tg C/yr)  | <b>Agriculture &amp; Waste*</b>               | <b>156.0±12.4</b> | <b>151.6±17.1</b> | <b>179.3±45.4</b> | <b>139.7±6.0</b>  | <b>168.8±26.4</b> | <b>151.6±9.0</b>  |
|                               | <b>Net CH<sub>4</sub> flux</b>                | <b>327.0±45.7</b> | <b>336.5±38.7</b> | <b>324.0±46.6</b> | <b>311.3±39.5</b> | <b>324.8±38.6</b> | <b>325.9±43.3</b> |
|                               | <b>Pre-industrial CH<sub>4</sub> emission</b> | <b>125.4±14.4</b> |                   |                   |                   |                   |                   |
|                               | <b>Human-induced CH<sub>4</sub> flux</b>      | <b>201.6±48.1</b> | <b>211.0±41.3</b> | <b>199.6±48.8</b> | <b>185.8±42.1</b> | <b>199.4±41.2</b> | <b>200.5±45.7</b> |
|                               | 1) Natural soil                               |                   | 7.9±1.3           | 6.6±0.5           | 8.2±1.3           | 7.5±0.4           | 8.4±0.9           |
|                               | 2) Biomass burning                            |                   | 0.7±0.1           | 0.7±0.1           | 0.7±0.1           | 0.6±0.1           | 0.6±0.2           |
|                               | 3) Agricultural soil                          |                   | 2.6±0.3           |                   | 3.3±0.2           |                   | 4.0±0.3           |
|                               | 4) Manure management                          |                   | 0.2±0.0           |                   | 0.2±0.0           |                   | 0.3±0.0           |
|                               | 5) Indirect emission                          |                   | 0.5±0.1           |                   | 0.9±0.1           |                   | 0.7±0.1           |
|                               | 6) Human Sewage                               |                   | 0.2±0.6           |                   | 0.2±0.0           |                   | 0.3±0.0           |
| N <sub>2</sub> O<br>(Tg N/yr) | <b>Agriculture &amp; Waste *</b>              |                   | 4.7±4.2           | 4.1±0.6           | 4.6±0.2           | 4.4±0.6           | 5.5±0.7           |
|                               | <b>Net N<sub>2</sub>O flux</b>                |                   | 14.0±4.3          | 11.3±0.8          | 14.3±0.9          | 12.6±0.7          | 15.2±1.0          |
|                               | <b>Pre-industrial N<sub>2</sub>O emission</b> | <b>7.4±1.3</b>    |                   |                   |                   |                   |                   |
|                               | <b>Human-induced N<sub>2</sub>O flux</b>      |                   | 6.6±4.5           | 3.9±1.5           | 6.9±1.6           | 5.2±1.5           | 7.8±1.6           |

Note: \* denotes that additional data are included in the calculation of greenhouse gas fluxes from this sub-total sector. Therefore, the sub-total GHG fluxes are not necessarily equal to the sum of individual sector values shown in this table. The complete set of data used for calculation could be found in supplementary Table S2.

720

721